Supporting Information for:

Building *trans*-Philicity (*trans*-Effect/*trans*-Influence) Ladders for Octahedral Complexes by NMR Probe

Athanassios C. Tsipis

Laboratory of Inorganic Chemistry, Department of Chemistry, University of Ioannina, Ioannina 45110, Greece

Table of Contents

Table S1. The isotropic σ ^{13}C shielding tensor elements and R(Cr-CO_{trans}) bond distances for octahedral $[Cr(CO)_5L]^{-/0/+}$ complexes calculated by the PBE0/Def2-TZVP(Cr) ∪ 6-31G(d,p)(E)/PCM and PBE0/Def2-TZVP(Cr) ∪ 6-311++G(d,p)(E)/PCM (figures in parentheses) computational protocols along with the ligand electronic parameters P_L and E_L(L).

Ligand	P_L (V)	E_L(L) (V)	R(Cr-C) (Å)	σ ^{13}C (ppm)	Ligand	P_L (V)	E_L(L) (V)	R(Cr-C) (Å)	σ ^{13}C (ppm)
N^+	1.46	1.94	2.412 (2.425)	19.41 (-0.58)	Br^-	-1.17	-0.22	1.817 ()1.816)	-25.07 (-52.76)
NO^+	1.40	1.90	2.015 (1.947)	4.42 (-17.45)	Cl^-	-1.15	-0.24	1.817 (1.816)	-23.96 (-51.05)
CO	0.30	0.99	1.898 (1.899)	-13.34 (-37.26)	F^-	-1.38	-0.42	1.822 (1.818)	-13.59 (-45.61)
N_2	-0.07	0.68	1.866 (1.862)	-15.90 (-41.54)	H^-	-1.22	-0.3	1.838 (1.838)	-26.22 (-54.25)
PH_3	-0.36	0.43	1.851 (1.851)	-20.06 (-45.85)	N_3^-	-1.26	-0.3	1.825 (1.823)	-21.53 (-48.57)
PMe_3	-0.47	0.33	1.846 (1.848)	-20.68 (-47.14)	OH^-	-1.55	-0.59	1.821 (1.819)	-16.41 (-45.73)
PPh_3	-0.35	0.39	1.847 (1.845)	-20.71 (-47.32)	SH^-	-1.35	-0.42	1.819(1.820)	-25.11 (-52.14)
PF_3	0.09	0.81	1.883 (1.886)	-16.10 (-40.49)	NH_2^-			1.820 (1.820)	-22.58 (-49.56)
CNH			1.875 (1.875)	-16.01 (-40.73)	Me^-	-1.88	-0.87	1.823 (1.825)	-27.17 (-54.5)
NCH	-0.39	0.4	1.849 (1.847)	-17.67(-43.63)	t-Bu^-	-1.91	-0.9	1.817 (1.817)	-26.63 (-54.51)
CNPh	-0.38	0.41	1.874 (1.874)	-16.76 (-41.83)	Ph^-	-1.59	-0.62	1.832 (1.834)	-25.28(-52.86)
NCPh	-0.40	0.37	1.847 (1.844)	-18.16 (-44.37)	$SnCl_3^-$			1.841 (1.841)	-25.29 (-52.63)
CNMe	-0.43	0.37	1.869 (1.868)	-17.03 (-41.90)	FO^-			1.832 (1.829)	-20.70 (-49.48)
NCMe	-0.58	0.34	1.845 (1.842)	-18.22 (-44.35)	ClO^-			1.827 (1.824)	-18.13 (-46.42)
Py	-0.59	0.25	1.838 (1.836)	-20.02 (-46.95)	BrO^-			1.826 (1.823)	-17.71 (-46.07)
NH_3	-0.77	0.07	1.835 (1.832)	-19.14 (-45.66)	$HCOO^-$	-1.21	-0.3	1.821 (1.819)	-21.69 (-49.31)
Carbene	-1.16	-0.26	1.851 (1.850)	-19.95 (-45.99)	CH_3COO^-			1.821 (1.819)	-21.64 (-49.27)
H_2O	-0.81	0.04	1.830 (1.826)	-21.33 (-48.99)	$CH_3CH_2COO^-$			1.821 (1.819)	-21.91 (-49.45)
H_2S	-0.36	0.43	1.838 (1.836)	-21.45 (-47.54)	$CH_3(CH_2)_2COO^-$			1.821 (1.819)	-21.87 (-49.40)
NO_3^-	-0.99	-0.11	1.826 (1.818)	-22.69 (-35.10)	$C_6H_5COO^-$			1.822 (1.820)	-21.73 (-49.24)
NO_2^-	-0.84	0.02	1.840 (1.838)	-20.90 (-48.47)	CH_2FCOO^-			1.822 (1.819)	-21.61 (-49.42)
NCS^-	-0.88	-0.06	1.834 (1.834)	-18.13 (-20.26)	CH_2ClCOO^-			1.822 (1.820)	-21.87 (-49.36)
SCN^-	-0.88	-0.06	1.824(1.824)	-24.10(-51.07)	CH_2BrCOO^-			1.822 (1.820)	-21.75 (-49.27)
CN^-	-1.00	0.02	1.844 (1.845)	-19.79 (-45.81)	$CHCl_2COO^-$			1.823 (1.821)	-21.74 ()
OCN^-	-1.16	-0.25	1.824 (1.820)	-21.38 (-49.45)	CCl_3COO^-			1.823 (1.821)	-21.92(-49.43)
					Reference			**1.825 (1.820)**	**-34.46 (-62.87)**

Table S2. The ν(Cr-CO_{trans}) (in cm^{-1}) and ν(C≡O_{trans}) (in cm^{-1}) stretching vigrational frequencies for octahedral $[Cr(CO)_5L]^{-/0/+}$ complexes calculated by the PBE0/Def2-TZVP(Cr) ∪ 6-31G(d,p)(E)/PCM and PBE0/Def2-TZVP(Cr) ∪ 6-311++G(d,p)(E)/PCM (figures in parentheses) computational protocols.

Ligand	ν(Cr-CO_{trans})	Ligand	ν(C≡O_{trans})	Ligand	ν(Cr-CO_{trans})	Ligand	ν(C≡O_{trans})
N^+	204.31 (198.93)	N^+	2315.37 (2313.46)	N_3^-	511.79 (507.66)	N_3^-	1974.27 (1941.54)
NO^+	332.26 (354.15)	NO^+	2239.43 (2176.69)	BrO^-	510.61 (506.17)	BrO^-	1963.26 (1929.20)
CO	410.84 (408.86)	CO	2113.94 (2057.90)	Br^-	517.89 (511.12)	Br^-	1971.71 (1941.23)
PF_3	464.45 (457.31)	PF_3	2095.58 (2087.23)	Cl^-	516.84 (513.43)	Cl^-	1970.06 (1938.07)
N_2	470.25 (468.25)	N_2	2068.05 (2042.41)	H^-	510.73 (504.88)	H^-	1960.37 (1919.66)
CNH	477.83 (471.27)	CNH	2058.10 (2033.04)	ClO^-	511.46 (507.64)	ClO^-	1963.64 (1930.67)
CNPh	469.65 (465.53)	CNPh	2056.51 (2032.33)	Ph^-	513.87 (507.81)	Ph^-	1957.05 (1923.49)
CNMe	478.42 (474.26)	CNMe	2049.22 (2023.30)	SH^-	517.65 (512.35)	SH^-	1964.19 (1931.46)
NCPh	487.44 (485.06)	NCPh	2026.62 (1996.39)	t-Bu^-	522.59 (518.25)	t-Bu^-	1937.26 (1903.94)
NCH	488.83 (485.67)	NCH	2032.23 (2003.81)	OH^-	526.22 (517.02)	OH^-	1944.46(1909.46)
NCMe	492.58 (490.07)	NCMe	2023.54 (1992.23)	F^-	527.74 (516.33)	F^-	1951.31 (1918.69)
PH_3	490.83 (487.19)	PH_3	2040.33 (2016.37)	NH_2^-	528.28 (520.33)	NH_2^-	1940.38 (1903.79)
PPh_3	496.08 (491.01)	PPh_3	2029.25 (2007.96)	Me^-	533.58 (525.07)	Me^-	1938.57 (1901.21)
PMe_3	496.29 (491.05)	PMe_3	2025.41 (2001.42)	NO_3^-	597.77 (512.64)	NO_3^-	1987.36 (1842.64
H_2S	495.03 (492.50)	H_2S	2026.96(1999.74)	CH_2FCOO^-	514.90 (510.81)	CH_2FCOO^-	1967.07 (1935.86)
Carbene	495.20 (491.14)	Carbene	2013.16 (1984.69)	CH_2ClCOO^-	512.87 (509.75)	CH_2ClCOO^-	1969.33 (1937.43)
Py	498.78 (496.13)	Py	2011.10 (1983.10)	CH_2BrCOO^-	513.07 (509.94)	CH_2BrCOO^-	1969.40 (1937.57)
$SnCl_3^-$	499.35 (498.75)	$SnCl_3^-$	2026.35 (2001.77)	$CHCl_2COO^-$	488.88 (514.83)	$CHCl_2COO^-$	1974.22 (1942.21)
H_2O	501.95 (500.31)	H_2O	2012.21 (1982.57)	CCl_3COO^-	491.84 (490.11)	CCl_3COO^-	1977.46 (1945.01)
NH_3	505.71 (503.20)	NH_3	2006.41 (1976.31)	$HCOO^-$	515.36 (511.09)	$HCOO^-$	1965.14 (1933.88)
CN^-	505.36(497.57)	CN^-	1994.51(1964.99)	CH_3COO^-	518.61 (516.07)	CH_3COO^-	1961.18 (1929.04)
NCS^-	505.60 (505.91)	NCS^-	1992.09 (1963.39)	$CH_3CH_2COO^-$	518.29 (515.42)	$CH_3CH_2COO^-$	1961.50 (1928.80)
NO_2^-	499.77 (493.58)	NO_2^-	1992.14 (1962.94)	$CH_3(CH_2)_2COO^-$	518.61 (516.23)	$CH_3(CH_2)_2COO^-$	1961.65 (1929.22)
FO-	508.83 (502.21)	FO-	1965.27 (1935.09)	$C_6H_5COO^-$	510.42 (507.48))	$C_6H_5COO^-$	1964.94 (1932.13)
OCN^-	509.76 (506.62)	OCN^-	1981.49 (1954.06)				
SCN^-	510.18 (505.97)	SCN^-	1984.08 (1958.78)				

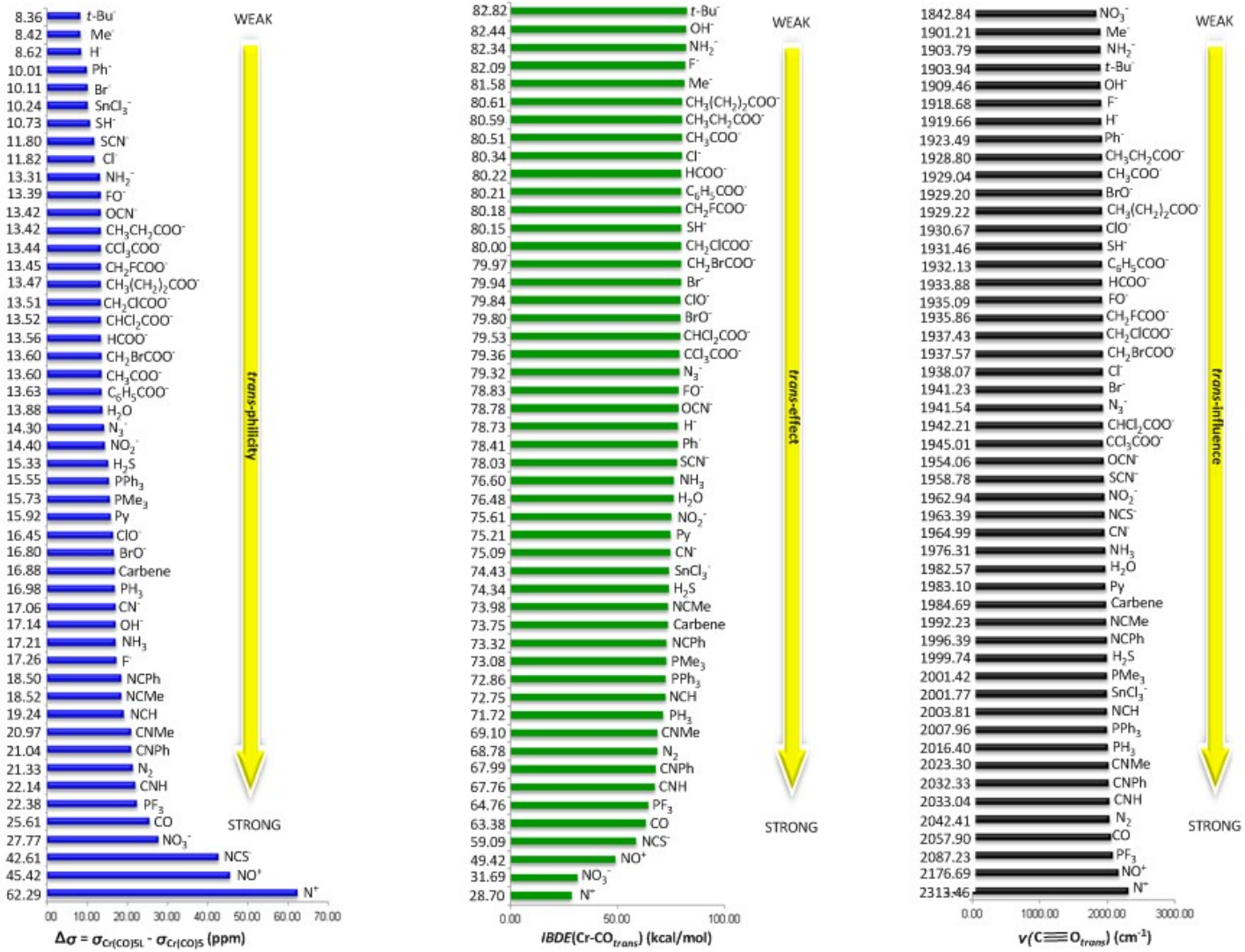

Chart S1. *Trans*-philicity, *trans*-effect and *trans*-influence ladders for octahedral $[Cr(CO)_5L]^{-/0/+}$ complexes quantified by $\Delta\sigma$ ^{13}C NMR, intrinsic bond dissociation energy of the Cr-CO_{trans} bond, *IBDE*(Cr-CO_{trans}) and the stretching vibrational frequency, $\nu(C{\equiv}O_{trans})$ probes respectively calculated by the PBE0/Def2-TZVP(Cr) ∪ 6-311++G(d,p)(E)/PCM computational protocol in dichloromethane solution.

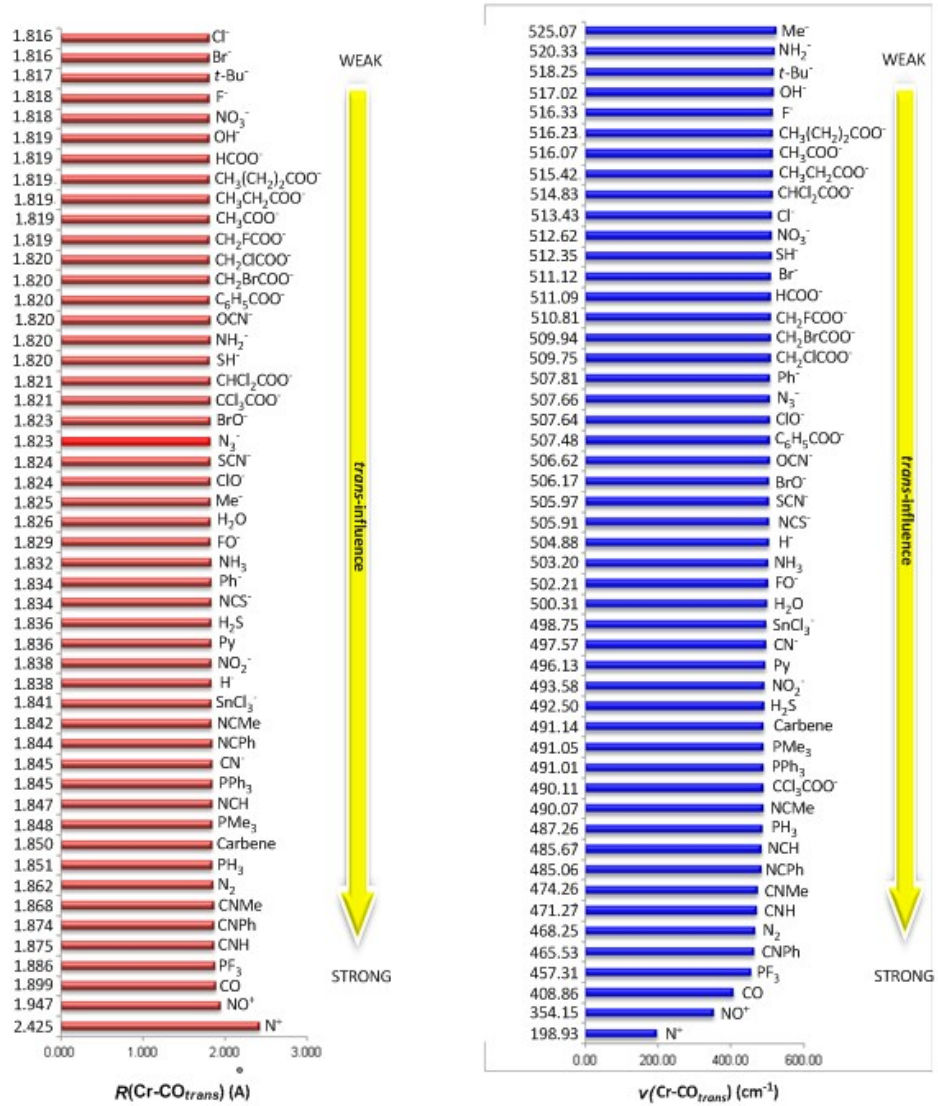

Chart S2. *Trans*-Influence ladders for octahedral $[Cr(CO)_5L]^{-/0/+}$ complexes quantified by the R(Cr-CO_{trans}) bond lengths and ν(Cr-CO_{trans}) vibrational frequencies calculated by the PBE0/Def2-TZVP(Cr) ∪ 6-311++G(d,p)(E)/PCM computational protocol in dichloromethane solution.

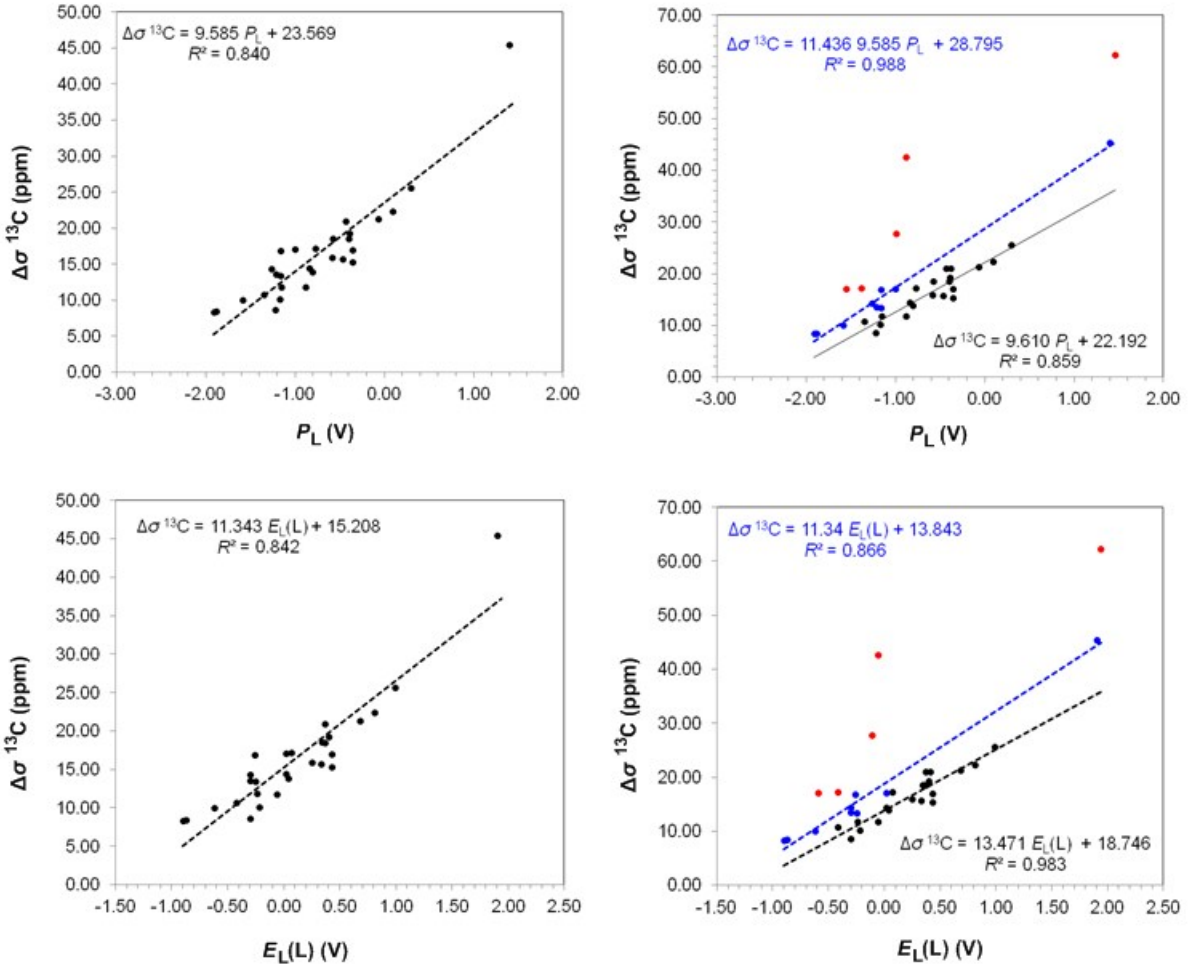

Figure S1. Linear relationships between σ_{calcd} ^{13}C shielding tensor elements of octahedral $[Cr(CO)_5L]^{-/0/+}$ complexes calculated by the GIAO/PBE0/Def2-TZVP(Cr) ∪ 6-311++G(d,p)(E)/PCM computational protocol and the P_L and $E_L(L)$ ligand electronic parameters.

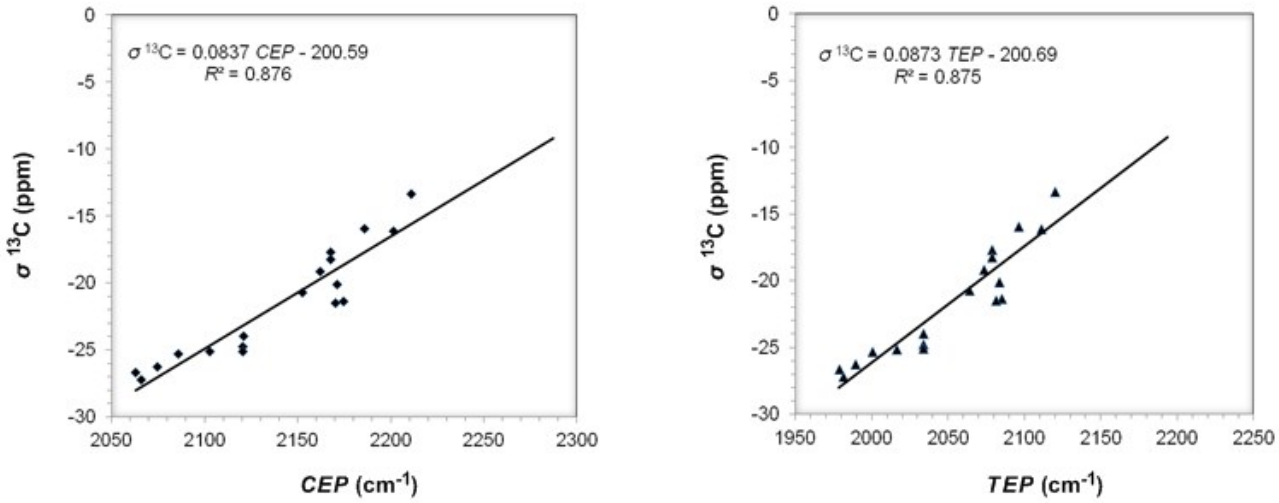

Figure S2. Linear relationships between σ_{calcd} ^{13}C shielding tensor elements of octahedral $[Cr(CO)_5L]^{-/0/+}$ complexes calculated by the GIAO/PBE0/Def2-TZVP(Cr) ∪ 6-31G(d,p)(E)/PCM computational protocol and the *CEP* and *TEP* ligand electronic parameters.

Table S3. Isotropic σ ^{13}C shielding tensor elements, Wiberg Bond orders, *WBO*(Cr-C), occupation of σ(Cr-CO$_{trans}$) and natural atomic charges Q_{Cr} and Q_C for octahedral $[Cr(CO)_5L]^{-/0/+}$ complexes calculated by the PBE0/Def2-TZVP(Cr) ∪ 6-31G(d,p)(E)/PCM computational protocol.

Ligand	*WBO*(Cr-C)	Occupation σ(Cr-CO$_{trans}$)	Q_{Cr}	Q_C	σ ^{13}C (ppm)	Ligand	*WBO*(Cr-C)	Occupation σ(Cr-CO$_{trans}$)	Q_{Cr}	Q_C	σ ^{13}C (ppm)
N^+	0.4946	1.94517	-1.97947	0.72128	19.41	$C_6H_5COO^-$	1.3086	1.92859	-2.66102	0.91379	-21.73
NO^+	0.8942	1.92516	-2.59868	0.94166	4.42	CH_2FCOO^-	1.3074	1.89355	-2.664	0.91400	-21.61
CO	1.0806	1.91268	-3.21695	0.97011	-13.34	CH_2ClCOO^-	1.3058	1.89367	-2.654	0.91500	-21.87
N_2	1.1554	1.90437	-2.88373	0.95996	-15.90	CH_2BrCOO^-	1.3053	1.89361	-2.65500	0.91500	-21.75
PH_3	1.1896	1.91137	-3.21842	0.96912	-20.06	CCl_3COO^-	1.3000	1.89355	-2.63800	0.91700	-21.92
PMe_3	1.2019	1.91050	-3.24197	0.96252	-20.68	NCS^-	1.2642	1.89953	-2.83262	0.93463	-18.13
PPh_3	1.2019	1.90227	-3.11676	0.96054	-20.71	SCN^-	1.2797	1.90604	-2.94001	0.94149	-24.10
CNH	1.1374	1.90876	-3.17012	0.96294	-16.01	CN^-	1.2338	1.91938	-3.16034	0.94451	-19.79
NCH	1.2078	1.90081	-2.84534	0.94900	-17.67	OCN^-	1.2945	1.89026	-2.60536	0.91708	-21.38
CNPh	1.1398	1.90855	-3.16103	0.96137	-15.89	Br^-	1.3097	1.90896	-2.88623	0.93448	-25.07
NCPh	1.2159	1.90029	-2.83827	0.94652	-18.16	Cl^-	1.3108	1.90694	-2.81871	0.92829	-23.96
CNMe	1.1591	1.90817	-3.16099	0.96083	-17.03	F^-	1.3192	1.88890	-2.61600	0.88800	-13.59
NCMe	1.2226	1.90023	-2.83534	0.94604	-18.22	H^-	1.2725	1.91790	-3.26664	0.91956	-26.22
Py	1.2025	1.89119	-2.73555	0.93793	-20.02	N_3^-	1.2907	1.90763	-2.80259	0.92428	-21.53
NH_3	1.2527	1.89426	-2.75059	0.93505	-19.14	OH^-	1.3212	1.89255	-2.73601	0.90118	-16.41
Carbene	1.1958	1.89968	-3.056	0.94600	-19.95	FO^-	1.2857	1.89521	-2.71457	0.90365	-20.70
H_2O	1.2633	1.89614	-2.58419	0.92609	-21.39	ClO^-	1.2980	1.89497	-2.68067	0.90667	-18.13
H_2S	1.2283	1.90657	-2.95736	0.95477	-21.45	BrO^-	1.2996	1.89479	-2.68059	0.90752	-17.71
PF_3	1.1056	1.91607	-3.47176	0.98343	-16.15	SH^-	1.3044	1.90949	-2.98265	0.93524	-25.11
NO_3^-	1.2902	1.89680	-2.66073	0.91927	-22.69	Ph^-	1.2646	1.89529	-3.00402	0.92107	-25.28
NO_2^-	1.2489	1.90086	-2.86156	0.92801	-20.90	Me^-	1.3095	1.90829	-3.04513	0.92409	-27.17
$HCOO^-$	1.3097	1.89429	-2.67107	0.91399	-21.69	*t*-Bu^-	1.3147	1.99686	-2.96384	0.92441	-26.63
$CH_3CH_2COO^-$	1.3125	1.89379	-2.666	0.91300	-21.91	NH_2^-	1.3188	1.91815	-2.87548	0.91466	-22.58
$CH_3(CH_2)_2COO^-$	1.3122	1.89375	-2.6654	0.91290	-21.87	$SnCl_3^-$	1.2087	1.91802	-3.42068	0.97586	-25.29
CH_3COO^-	1.3123	1.89378	-2.669	0.91400	-21.64						

Table S4. Wiberg Bond orders, *WBO*(Cr-C), occupation of σ(Cr-CO_{trans}) and natural atomic charges Q_{Cr} and Q_C for octahedral $[Cr(CO)_5L]^{-/0/+}$ complexes calculated by the PBE0/Def2-TZVP(Cr) ∪ 6-311++G(d,p)(E)/PCM computational protocol.

Ligand	*WBO*(Cr-C)	Occupation σ(Cr-CO_{trans})	Q_{Cr}	Q_C	Ligand	*WBO*(Cr-C)	Occupation σ(Cr-CO_{trans})	Q_{Cr}	Q_C
N^+	0.50100	1.9473	-2.00749	0.7069	$C_6H_5COO^-$	1.30800	1.92207	-2.69534	0.93664
NO^+	0.97830	1.92249	-2.64463	0.9624	CH2FCOO	1.30680	1.88786	-2.69178	0.93745
CO	1.07850	1.90638	-3.28233	0.98794	$CHCl_2COO$	1.30040	1.88806	-2.68539	0.93889
N_2	1.16450	1.89948	-2.9304	0.97831	CH_2ClCOO^-	1.30540	1.8879	-2.68943	0.93751
PH_3	1.18550	1.90335	-3.27093	0.99006	CH_2BrCOO^-	1.30490	1.88788	-2.68912	0.93754
PMe_3	1.18890	1.89766	-3.30925	0.98561	CCl_3COO^-	1.29930	1.88791	-2.67697	0.9392
PPh_3	1.19100	1.89127	-3.22832	0.98643	NCS^-	1.26580	1.89534	-2.83783	0.9496
CNH	1.21330	1.89718	-2.8946	0.96772	SCN^-	1.27440	1.89805	-2.99321	0.96421
NCH	1.13790	1.90195	-3.22518	0.98036	CN^-	1.22640	1.90045	-3.22775	0.96811
CNPh	1.22080	1.89616	-2.88598	0.96518	OCN^-	1.29700	1.88549	-2.63031	0.93847
NCPh	1.15340	1.90103	-3.22391	0.98007	Br^-	1.26030	1.90365	-2.91505	0.95585
CNMe	1.22820	1.89584	-2.88321	0.96482	Cl^-	1.30800	1.90124	-2.86732	0.9504
NCMe	1.24240	1.88486	-2.78843	0.95825	H^-	1.26670	1.90837	-3.35687	0.94653
Py	1.25680	1.88848	-2.79518	0.95517	N_3^-	1.29130	1.90041	-2.84124	0.94727
NH_3	1.19930	1.88983	-3.12026	0.96747	OH^-	1.32250	1.89052	-2.73279	0.92499
Carbene	1.13520	1.9027	-3.23846	0.98205	F^-	1.32540	1.88975	-2.58986	0.91473
H_2O	1.26990	1.89194	-2.61012	0.94466	FO^-	1.28590	1.89046	-2.73271	0.92943
H_2S	1.22960	1.89938	-3.00979	0.97485	ClO^-	1.30010	1.88994	-2.7027	0.93041
PF_3	1.08880	1.90525	-3.50402	1.00291	BrO^-	1.30130	1.8903	-2.69746	0.9304
NO_3^-	1.30180	1.88803	-2.58683	0.90168	SH^-	1.29680	1.90211	-3.04599	0.95935
NO_2^-	1.25010	1.89374	-2.89765	0.9525	Ph^-	1.25060	1.88461	-3.06829	0.9452
$HCOO^-$	1.30860	1.88832	-2.70152	0.93725	Me^-	1.29820	1.90045	-3.10566	0.9498
$CH_3CH_2COO^-$	1.31110	1.88781	-2.70029	0.93597	*t*-Bu^-	1.29720	1.87921	-3.03078	0.95323
$CH_3(CH_2)_2COO^-$	1.31100	1.88782	-2.69896	0.93576	NH_2^-	1.31360	1.89359	-2.90623	0.93727
CH_3COO^-	1.31110	1.88781	-2.70043	0.9359	$SnCl_3^-$	1.20080	1.90714	-3.48697	0.99588

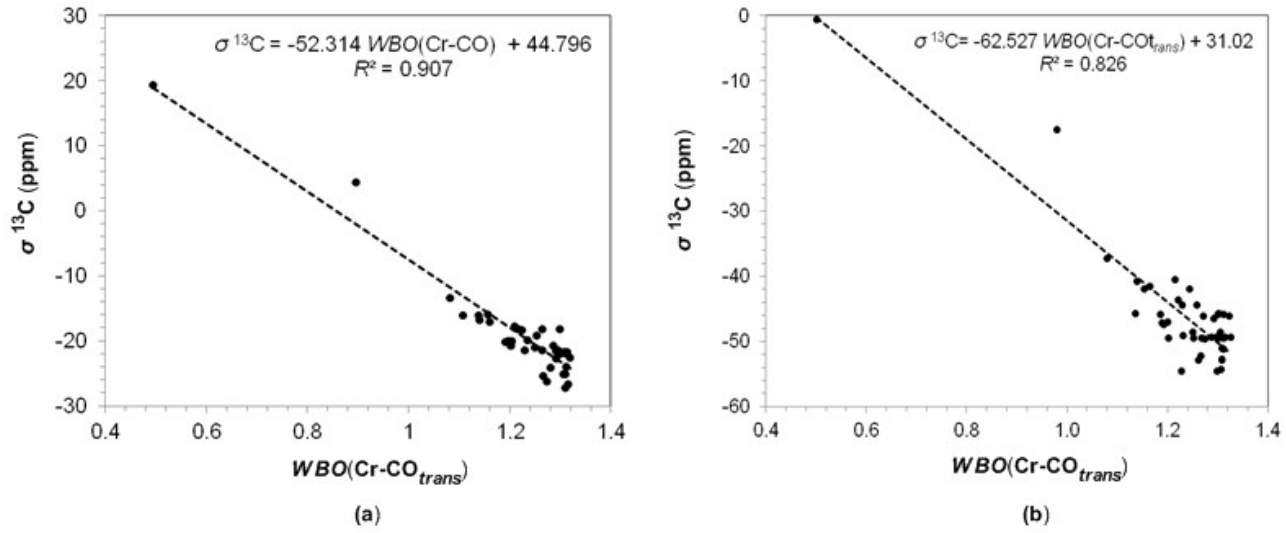

Figure S3. Linear plot of σ_{calcd} ^{13}C vs *WBO*(Cr-CO_{trans}) of octahedral $[Cr(CO)_5L]^{-/0/+}$ complexes calculated by the GIAO/PBE0/Def2-TZVP(Cr) ∪ 6-31G(d,p)(E)/PCM (**a**) and GIAO/PBE0/Def2-TZVP(Cr) ∪ 6-311++G(d,p)(E)/PCM (**b**) computational protocols.

Table S5. The 4*s*(%), 4*p*(%) and 3*d*(%) character of the *spd* hybridized orbitals of the Cr metal center used in the Cr-CO_{trans} bonding calculated by the PBE0/Def2-TZVP(Cr) ◡ 6-31G(d,p)(E)/PCM and PBE0/Def2-TZVP(Cr) ◡ 6-311++G(d,p)(E)/PCM (figures in parentheses) computational protocols.

Ligand	4*s*%	4*p*%	3*d*%	Ligand	4*s*%	4*p*%	3*d*%
N^+	8.41 (9.10)	69.33 (68.96)	22.23 (21.92)	Br^-	17.72 (17.88)	47.59 (47.54)	34.68 (34.58)
NO^+	13.48 (17.54)	55.27 (48.46))	31.23 (34.00)	Cl^-	17.43 (17.57)	48.17 (48.15)	34.39 (34.27)
CO	16.67 (16.67)	49.99 (49.99)	33.33 (33.33)	F^-	15.35 (16.16)	52.95 (52.29)	31.68 (31.54)
N_2	16.07 (16.19)	50.11 (49.5)	33.81 (34.05)	H^-	20.09 (20.07)	48.5 (48.57)	31.40 (31.35)
PH_3	18.18 (18.12)	46.34(46.63)	35.47(35.25)	N_3^-	16.22 (17.48)	44.17 (47.13)	35.54 (35.38)
PMe_3	18.38 (18.11)	46.45 (46.72)	35.16 (35.16)	OH^-	16.17 (16.64)	52.58 (52.11)	31.24 (31.24)
PPh_3	17.25(17.27)	46.49 (46.79)	36.26 (35.93)	SH^-	18.08 (18.15)	48.02 (48.19)	33.89 (33.66)
PF_3	18.04 (17.78)	45.52 (45.60)	36.43 (36.61)	NH_2^-	17.45 (17.75)	51.02 (51.24)	31.51 (31.00)
CNH	17.01 (17.07)	49.73 (49.75)	33.25 (33.18)	Me^-	18.96 (19.14)	49.72 (49.98)	31.32 (30.87)
NCH	16.29 (16.52)	50.23 (49.83)	33.48 (33.64)	t-Bu^-	17.78 (17.69)	49.12 (50.26)	33.09(32.04)
CNPh	17.01 (17.04)	49.79 (49.81)	33.20 (33.14)	Ph^-	17.99 (18.01)	49.94(50.11)	32.06 (31.87)
NCPh	16.29 (16.50)	50.27 (49.94)	33.42 (33.55)	OF-	16.02 (16.27)	52.54 (52.32)	31.42 (31.41)
CNMe	17.13 (17.13)	49.55 (49.59)	33.31 (33.27)	ClO^-	16.05 (16.29)	51.84 (51.55)	32.10 (32.15)
NCMe	16.42 (16.55	50.06 (49.82)	33.51 (33.63)	BrO^-	16.04 (16.27)	51.72 (51.36)	32.23 (32.37)
Py	15.79 (15.92)	51.45 (51.32)	32.75 (32.75)	$HCOO^-$	16.05 (16.24)	51.29 (51.16)	32.65 (32.59)
NH_3	16.16 (16.26)	51.01 (50.87)	32.82 (32.86)	CH_3COO^-	16.02 (16.28)	51.39 (51.26)	32.57 (32.45)
Carbene	17.21 (17.09)	49.94 (50.07)	32.85 (32.84)	$CH_3CH_2COO^-$	16.02 (16.29)	51.36 (51.21)	32.60 (32.49)
H_2O	16.00 (16.23)	50.12 (49.93)	33.87 (33.83)	$CH_3(CH_2)_2COO^-$	16.01 (16.28)	51.36 (51.23)	32.61 (32.48)
H_2S	17.32 (17.23)	47.19 (47.51)	35.47 (35.25)	$C_6H_5COO^-$	23.58 (23.70)	28.66 (29.06)	47.76 (47.23)
NO_3^-	16.07 (16.24)	50.64 (50.45)	33.28 (33.29)	CH_2FCOO^-	16.00 (16.24)	51.43 (51.17)	32.56 (32.58)
NO_2^-	16.63 (16.61)	51.23 (50.89)	32.13 (32.49)	CH_2ClCOO^-	15.99 (16.23)	51.35 (51.15)	32.65 (32.61)
NCS^-	16.59 (16.86)	50.05(49.86)	33.34 (33.27)	CH_2BrCOO^-	15.98 (16.23)	51.37 (51.15)	32.64 (32.61)
SCN^-	17.51 (17.46)	48.09 (48.39)	34.39 (34.14)	$CHCl_2COO^-$	15.96 (16.21)	51.32 (51.14)	32.71 (32.64)
CN^-	17.84 (17.94)	48.75 (48.86)	33.39 (33.20)	CCl_3COO^-	15.95 (16.18)	51.34 (51.14)	32.69 (32.67)
OCN^-	15.81 (16.02)	52.04 (51.87)	32.14 (32.10)	$SnCl_3^-$	19.57 (19.20)	44.20 (44.65)	36.22 (36.14)

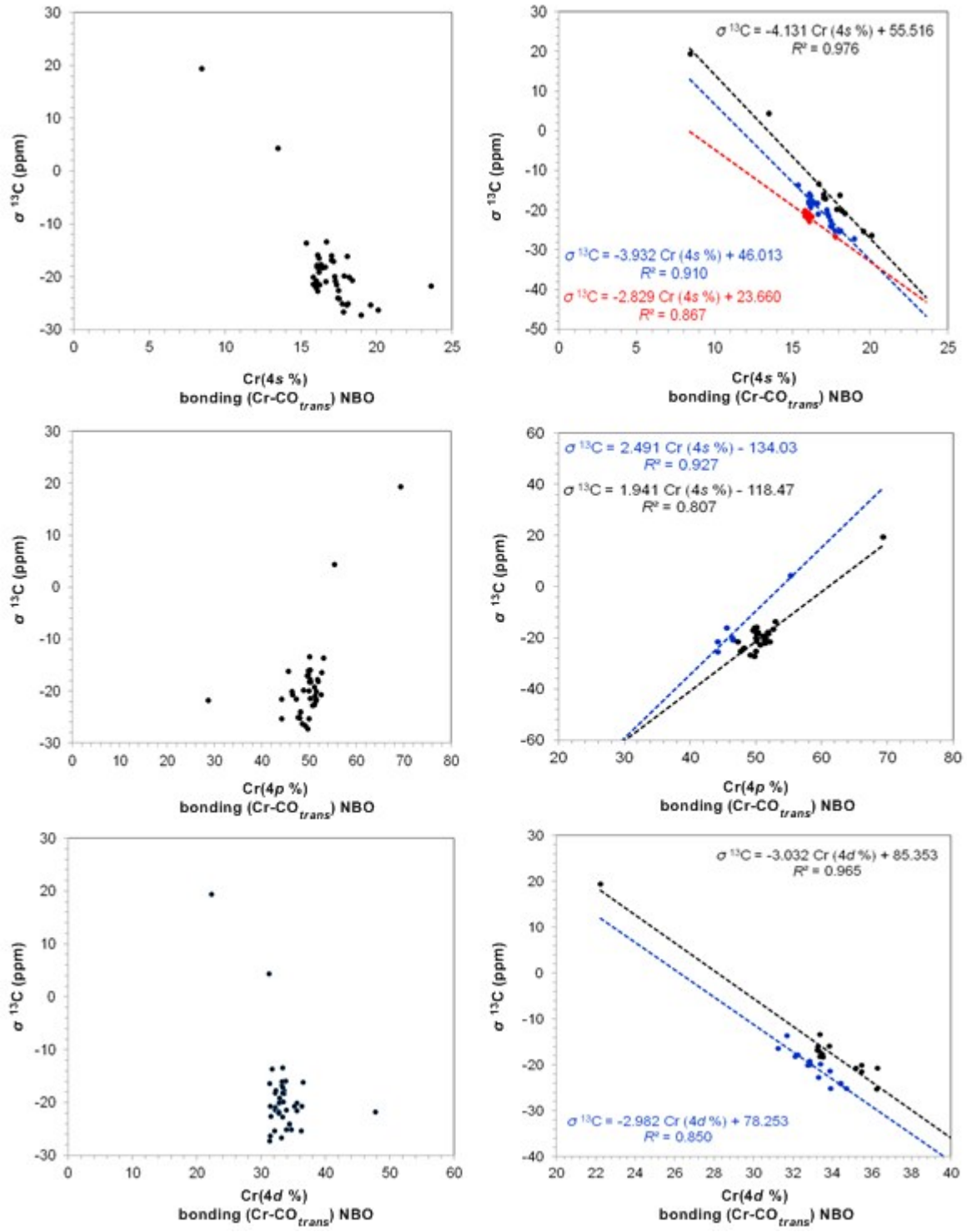

Figure S4. Plots of σ_{calcd} ^{13}C *vs* Cr(4*s*%), σ_{calcd} ^{13}C *vs* Cr(4*p*%) and σ_{calcd} ^{13}C *vs* Cr(3*d*%) character of the bonding σ(Cr-CO$_{trans}$) natural bond orbital of octahedral $[Cr(CO)_5L]^{-/0/+}$ complexes calculated by the GIAO/PBE0/Def2-TZVP(Cr) ∪ 6-31G(d,p)(E)/PCM computational protocol.

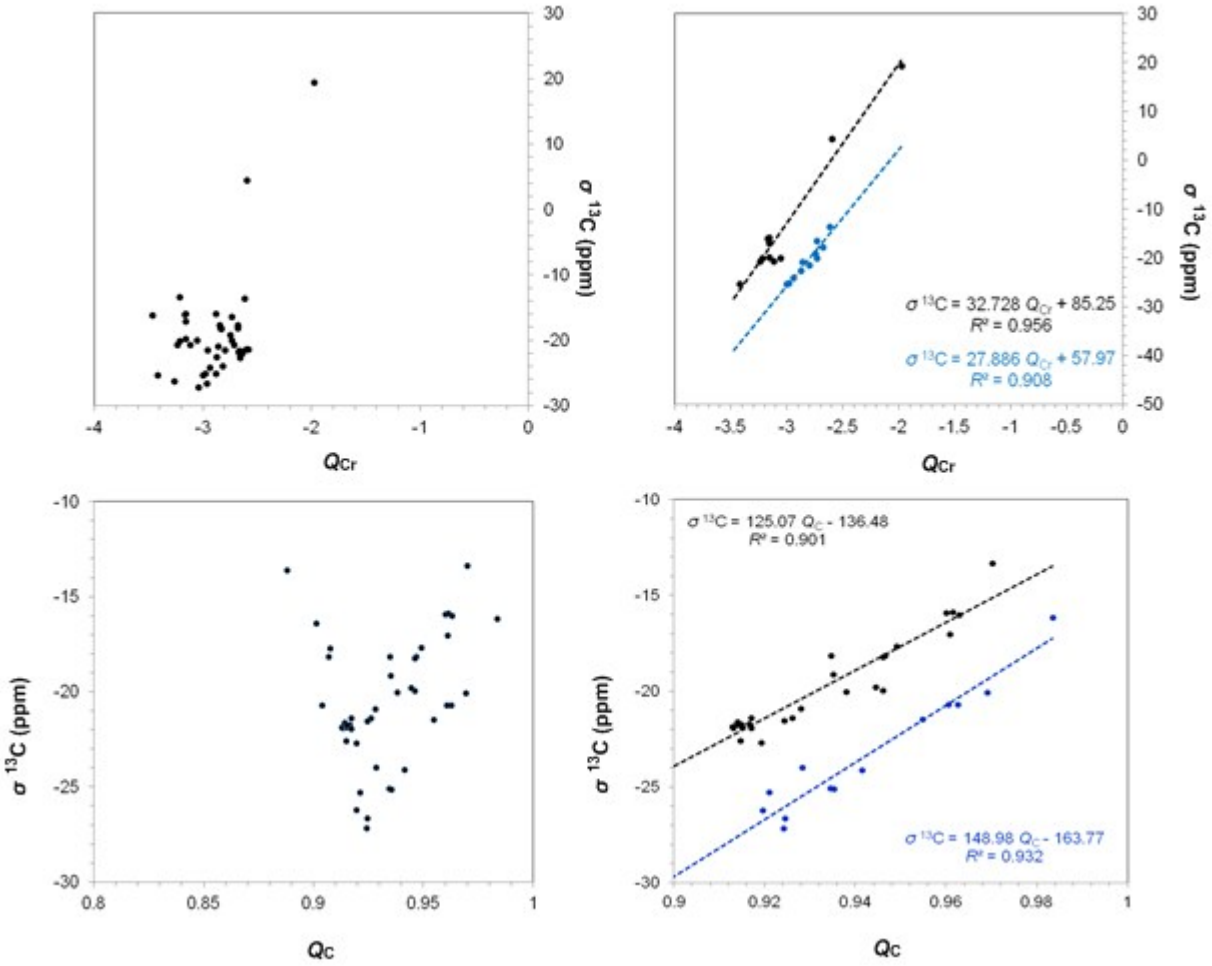

Figure S5. Plots of σ_{calcd} ^{13}C *vs* Q_{Cr} and σ_{calcd} ^{13}C *vs* Q_C of octahedral $[Cr(CO)_5L]^{-/0/+}$ complexes calculated by the GIAO/PBE0/Def2-TZVP(Cr) ∪ 6-31G(d,p)(E)/PCM computational protocol.

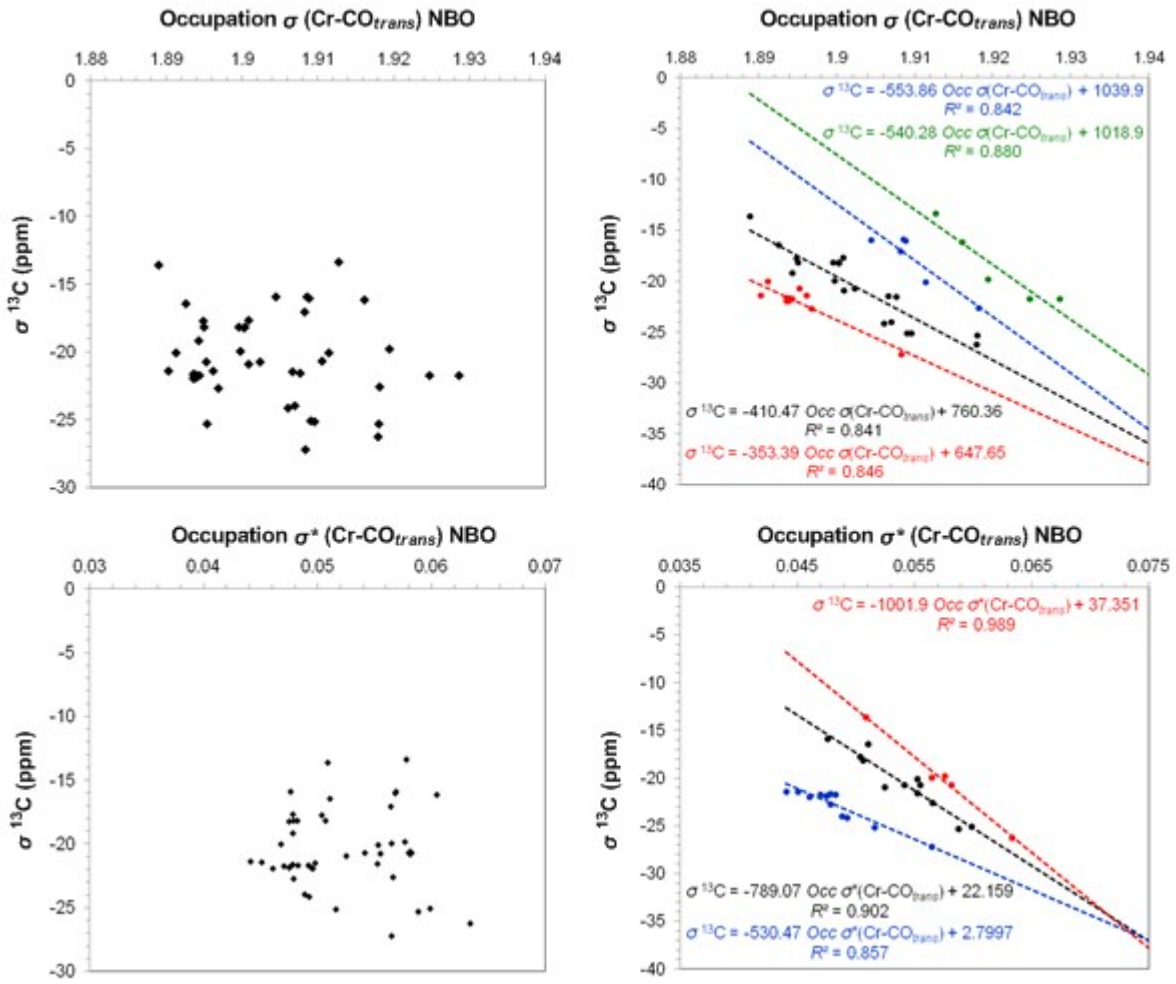

Figure S6. Plots of σ_{calcd} ^{13}C *vs Occupation of* σ(Cr-CO$_{trans}$) and σ_{calcd} ^{13}C *vs Occupation of* σ*(Cr-CO$_{trans}$) NBOs of octahedral $[Cr(CO)_5L]^{-/0/+}$ complexes calculated by the GIAO/PBE0/Def2-TZVP(Cr) ∪ 6-31G(d,p)(E)/PCM computational protocol.